J|A|C|S
ARTICLES
Published on Web 04/10/2002

Synthesis, Characterization, and Spectroscopy of 4,7,12,15-[2.2]Paracyclophane Containing Donor and Acceptor Groups: Impact of Substitution Patterns on Through-Space Charge Transfer

Glenn P. Bartholomew and Guillermo C. Bazan*

Contribution from the Departments of Chemistry and Materials and Institute for Polymers and Organic Solids, University of California, Santa Barbara, California 93106

Received September 6, 2001. Revised Manuscript Received February 8, 2002

Abstract: This paper reports the synthesis of 4,7,12,15-tetra(4′-dihexylaminostyryl)[2.2]paracyclophane (**1**), 4-(4′-dihexylaminostyryl)-7,12,15-tri(4″-nitrostyryl)[2.2]paracyclophane (**2**), 4,7-bis(4′-dihexylaminostyryl)-12,15-bis(4″-nitrostyryl)-[2.2]paracyclophane (**3**), 4,7,12-tris(4′-dihexylaminostyryl)-15-(4″-nitrostyryl)[2.2]-paracyclophane (**4**), 4,15-bis(4′-dihexylaminostyryl)-7,12-bis(4″-nitrostyryl)[2.2]paracyclophane (**5**), and 4,12-bis(4′-dihexylaminostyryl)-7,15-bis(4″-nitrostyryl)[2.2]paracyclophane (**6**). These molecules represent different combinations of bringing together distyrylbenzene chromophores containing donor and acceptor groups across a [2.2]paracyclophane (pCp) bridge. X-ray diffraction studies show that the lattice arrangements of **1** and **3** are considerably different from those of the parent chromophores 1,4-bis(4′dihexylaminostyryl)-benzene (DD) and 1,4-di(4′-nitrostyryl)benzene (AA). Differences are brought about by the constraint by the pCp bridge and by virtue of chirality in the "paired" species. The absorption and emission spectra of **1**−**6** are also presented. Clear evidence of delocalization across the pCp structure is observed. Further, in the case of **2**, **3**, and **4**, emission from the second excited state takes place.

Introduction

Through-space delocalization between optically and electronically active organic molecules constitutes a broad area of chemical research. In the area of optoelectronic materials, the charge transport ability and optical performance are controlled by the spatial relationship between molecules that form the bulk material.[1−3] Substantial efforts to control the distance and orientation between molecular subunits[4,5] have resulted in novel functions and properties such as organic injection lasers[6] and superconductivity.[7] The function of important biological processes such as photosynthesis[8] and oxidative DNA damage[9] depends on energy transfer processes between organic subunits. Optical signatures have been used to characterize the geometry and phase transitions of gas-phase van der Waals clusters.[10] Defining the extent of molecule−molecule interactions in conjugated molecules with precise dimensions,[11] and controlling these interactions, will also bear an influence on the area of molecular electronics.[12,13]

Molecules built around the [2.2]paracyclophane (pCp) skeleton[14] have proven useful for studying chromophore−chromophore interactions.[15] Some of these structures are designed to mimic through-space delocalization in conjugated organic materials.[16,17] Others probe intramolecular charge transfer (ICT) across the transannular gap and thus the properties of donor/acceptor groups separated through space.[18] In this context, 4-(4′-dihexylaminostyryl)-16-(4″-nitrostyryl)-[2.2]paracyclophane (4D-16A-pCp) was recently synthesized, and its optical and nonlinear optical properties were correlated against theoretical analysis.[19]

* To whom correspondence should be addressed. E-mail: bazan@chem.ucsb.edu.

(1) Li, X.-C.; Sirringhaus, H.; Garnier, F.; Holmes, A. B.; Moratti, S. C.; Feeder, N.; Clegg, W.; Teat, S. J.; Friend, R. H. *J. Am. Chem. Soc.* **1998**, *120*, 2206.
(2) McGehee, M. D.; Bergstedt, T.; Zhang, C.; Saab, A. P.; O'Regan, M. B.; Bazan, G. C.; Srdanov, V. I.; Heeger, A. J. *Adv. Mater.* **1999**, *11*, 1349.
(3) Pope, M.; Swenberg, C. E. *Electronic Processes in Organic Crystals*; Clarendon Press: New York, 1982.
(4) Desiraju, G. R. In *Comprehensive Supramolecular Chemistry, Solid-State Supramolecular Chemistry: Crystal Engineering*; Atwood, J. L., Davies, J. E. D., Macnicol, D. D., Vögtle, F., Eds.; Pergamon Press: Exeter, U.K., 1996; Vol. 6, pp 1−22 and references therein.
(5) Selected examples: (a) Li, X.-C.; Sirringhaus, H.; Garnier, F.; Holmes, A. B.; Feeder, S. C.; Clegg, W.; Teat, S. M.; Friend, R. H. *J. Am. Chem. Soc.* **1998**, *120*, 2206. (b) Shetty, A. S.; Liu, E. B.; Lachicotte, R. J.; Jenekhe, S. A. *Chem. Mater.* **1999**, *11*, 2292. (c) Wu. G.; Jacobs, S.; Lenstra, A. T. H.; Van Alsenoy, C.; Geise, H. J. *J. Comput. Chem.* **1996**, *17*, 1820. (d) Van Hutton, P. F.; Wildeman, J.; Meetsma, A.; Hadziioannou, G. *J. Am. Chem. Soc.* **1999**, *121*, 5910.
(6) Schon, J. H.; Kloc, C.; Dodabalapur, A.; Batlogg, B. *Science* **2000**, *289*, 599.
(7) Schon, J. H.; Dodabalapur, A.; Bao, Z.; Kloc, C.; Schenker, O.; Batlogg, B. *Nature* **2001**, *410*, 189.
(8) (a) Special issue on Light-Harvesting Physics Workshop. *J. Phys. Chem. B* **1997**, *101*. (b) Sundström, V.; van Grondelle, R. In *Anoxygeneic Photosynthetic Bacteria*; Blankenship, R. E., Madiga, M. T., Baner, C. E., Eds.; Kluwer Academic: Dordrecht, 1995; p 349. (c) Hu, X.; Damjanovic, A.; Ritz, T.; Schulten, K. *Proc. Natl. Acad. Sci. U.S.A.* **1998**, *95*, 5935. (d) Linnanto, J.; Helenius, V. M.; Oksanen, J. A. I.; Peltola, T.; Garaud, J.-L.; Korppi-Tommola, J. E. I. *J. Phys. Chem. A* **1998**, *102*, 4337.
(9) (a) Lewis, F. D.; Letsinger, R. L.; Wasielewski, M. R. *Acc. Chem. Res.* **2001**, *34*, 159. (b) Armitage, B. *Chem. Rev.* **1998**, *98*, 1171. (c) Meggers, E.; Michel-Beyerle, M. E.; Giese, B. *J. Am. Chem. Soc.* **1998**, *120*, 12950.
(10) (a) Lim, E. C.; Saigusa, H. *Acc. Chem. Res.* **1996**, *29*, 129. (b) Kim, K. S.; Tarakeshwar, P.; Lee, J. Y. *Chem. Rev.* **2000**, *100*, 4145.
(11) (a) Robinson, M. R.; Wang, S.; Bazan, G. C.; Cao, Y. *Adv. Mater.* **2000**, *12*, 1701. (b) Renak, M.; Bartholomew, G. P.; Wang, S.; Ricatto, P. J.; Lachicotte, R. J.; Bazan, G. C. *J. Am. Chem. Soc.* **1999**, *121*, 7787.
(12) Sheats, J. R.; Barbara, P. F. *Acc. Chem. Res.* **1999**, *32*, 191.
(13) Goldhaber-Gordon, D.; Montemerlo, M. S.; Love, C.; Opiteck, G. J.; Ellenbogen, J. C. *Proc. IEEE* **1997**, *85*, 521.
(14) Voegtle, F. *Cyclophane Chemistry*; Wiley & Sons: New York, 1993.

Scheme 1

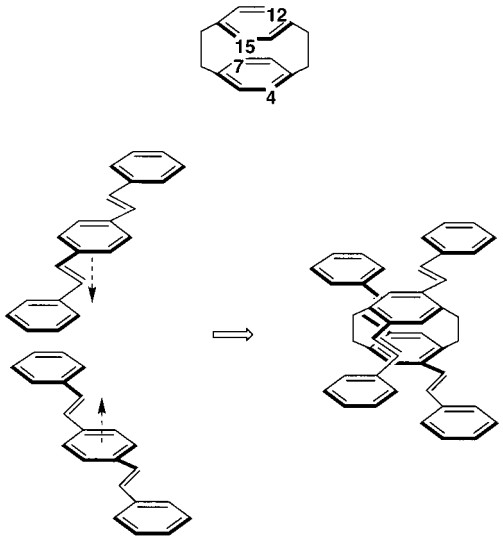

Unambiguous "through-space" charge transfer was evident by the 3-fold increase of β_{EFISH} for 4D-16A-pCp relative to the additive parallel superposition of the corresponding substituted stilbenes the pCp interconnects.[20] This increase in nonlinear efficiency was not accompanied by the usual red-shift in the absorption spectrum commonly seen with typical D/A through-bond coupling schemes.

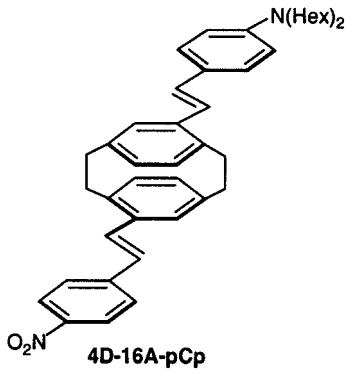

4D-16A-pCp

Within 4D-16A-pCp, the ICT is mediated by the $\pi-\pi$ stack, defined by the pCp core, and is unidirectional, from the dihexylamino group to the nitro functionality. In this contribution, we turn our attention to pCp chromophores with more complex combinations of donor and acceptor groups. These molecules may show multidirectional ICT states. Conceptually, our molecular design involves bringing together distyrylbenzene chromophores with their cofacial contact defined by the 4,7,-12,15-tetrasubstitution pattern in pCp (Scheme 1). The three parent distyrylbenzene chromophores are 1,4-bis(4′dihexylaminostyryl)benzene (DD), 1-(4′-dihexylaminostyryl)-4-(4″-nitrostryl)-benzene (DA), and 1,4-di(4′-nitrostyryl)benzene (AA).

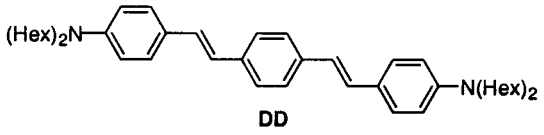

DD

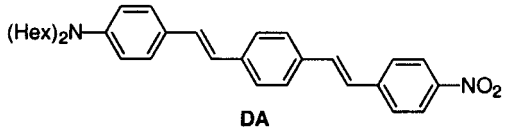

DA

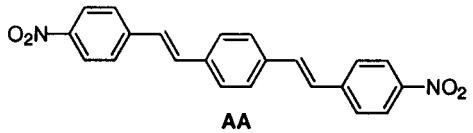

AA

Of the seven possible unique AA, DD, DA combinations, six are presented in this contribution (Scheme 2). With four donor groups, 4,7,12,15-tetra(4′-dihexylaminostyryl)[2.2]paracyclophane (**1**) can be viewed as the pairing of two DD chromophores. For 4-(4′-dihexylaminostyryl)-7,12,15-tri(4″-nitrostyryl)[2.2]paracyclophane (**2**) and 4,7,12-tris(4′-dihexylaminostyryl)-15-(4″-nitrostyryl)[2.2]paracyclophane (**4**), a dipolar DA chromophore is matched with a symmetrical acceptor (AA) and donor unit (DD), respectively. Molecule 4,7-bis-(4′-dihexylaminostyryl)-12,15-bis(4″-nitrostyryl)[2.2]paracyclophane (**3**) represents a close contact between AA and DD. In 4,15-bis(4′-dihexylaminostyryl)-7,12-bis(4″-nitrostyryl)[2.2]-paracyclophane (**5**) and 4,12-bis(4′-dihexylaminostyryl)-7,15-bis(4″-nitrostyryl)[2.2]paracyclophane (**6**), we see two different orientations for the overlap of two DA chromophores. The seventh permutation, (4,7,12,15)tetra(4′-nitrostyryl)[2.2]paracyclophane, is excluded from the study due to its extraordinary insolubility.

In addition to the synthesis of **1**−**6**, we present a study of the impact on the solid-state arrangements by the covalent constraint introduced by pCp, relative to the individual chromophores. The linear spectroscopy of **1**−**6** is also presented and reveals competing relaxations between the first and second excited states. The evaluation of the (4,7,12,15)-substitution pattern in the design of multipolar nonlinear optical chromophores will be published elsewhere.[21]

(15) Chromophores studied in this manner include: (a) phenanthrenophane, Schweitzer, D.; Hausser, K. H.; Haenel, M. *Chem. Phys.* **1978**, *29*, 181. (b) anthracenophane, Ishikawa, S.; Nakamura, J.; Iwata, S.; Sumitami, M.; Nagakura, S.; Sakata, Y.; Misumi, S. *Bull. Chem. Soc. Jpn.* **1979**, *52*, 1346. (c) fluorenophane, Haenel, M. W. *Tetrahedron Lett.* **1976**, *36*, 3121. (d) Colpa, J. P.; Hausser, K. H.; Schweitzer, D. *Chem. Phys.* **1978**, *29*, 187. (e) pyrenophane and several isomers of naphthalenophane, Haenel, M.; Staab, H. A. *Chem. Ber.* **1973**, *106*, 2190. Otsubo, T.; Mizogami, S.; Osaka, N.; Sakata, Y.; Misumi, S. *Bull. Chem. Soc. Jpn.* **1977**, *50*, 1858−1862. (f) stilbenophanes, Anger, I.; Sandros, K.; Sundahl, M.; Wennerström, O. Cis−Trans Photoisomerization of Bis-stilbenes with Ethylene Bridges. *J. Phys. Chem.* **1993**, *97*, 1920−1923. Tsuge, A.; Nishimoto, T.; Uchida, T.; Yasutake, M.; Moriguchi, T.; Sakata, K. Synthesis of Small-Sized Stilbenophanes and Their Transannular Delocalization. *J. Org. Chem.* **1999**, *64*, 7246−7248.

(16) (a) Bartholomew, G. P.; Bazan, G. C. *Acc. Chem. Res.* **2001**, *34*, 30. (b) Oldham, W. J.; Miao, Y.-J.; Lachicotte, R. J.; Bazan, G. C. *J. Am. Chem. Soc.* **1998**, *120*, 419. (c) Bazan, G. C.; Oldham, W. J.; Lachicotte, R. J.; Tretiak, S.; Chernyak, V.; Mukamel, S. *J. Am. Chem. Soc.* **1998**, *120*, 9188.

(17) (a) Wang, S.; Bazan, G. C.; Tretiak, S.; Mukamel, S. *J. Am. Chem. Soc.* **2000**, *122*, 1289. (b) Verdal, N.; Goodbout, J. T.; Perkins, T. L.; Bartholomew, G. P.; Bazan, G. C.; Myers-Kelly, A. *Chem. Phys. Lett.* **2000**, *320*, 95.

(18) (a) Staab, H. A.; Rebafka, W. *Chem. Ber.* **1977**, *110*, 3333. (b) Staab, H. A.; Haffner, H. *Chem. Ber.* **1977**, *110*, 3358. (c) Staab, H. A.; Starker, B.; Krieger, C. *Chem. Ber.* **1983**, *116*, 3831. (d) Staab, H. A.; Schanne, L.; Krieger, C.; Weiser, J.; Tagliever, V. *Chem. Ber.* **1985**, *118*, 1204. (e) Tashiro, M.; Koya, K.; Yamato, T. *J. Am. Chem. Soc.* **1983**, *105*, 6650. (f) Machida, H.; Tatemitsu, H.; Sakata, Y.; Misumi, S. *Tetrahedron Lett.* **1978**, 915. (g) Review: Keehn, P. M. In *Cyclophanes*; Keehn, P. M., Rosenfeld, S. M., Eds.; Academic Press: New York, 1983. (h) Review: Schwartz, M. H. *J. Inclusion Phenom. Mol. Recognit. Chem.* **1990**, *9*, 1.

(19) Zyss, J.; Ledoux, I.; Volkov, S.; Chernyak, V.; Mukamel, S.; Bartholomew, G. P.; Bazan, G. C. *J. Am. Chem. Soc.* **2000**, *122*, 11956.

(20) For a discussion on hyperpolarizability as a sensitive measure of intramolecular charge-transfer, see: Zyss, J. *J. Chem. Phys.* **1979**, *71*, 446.

(21) Bartholomew, G. P.; Ledoux, I.; Zyss, J.; Bazan, G. C., unpublished work.

Scheme 2

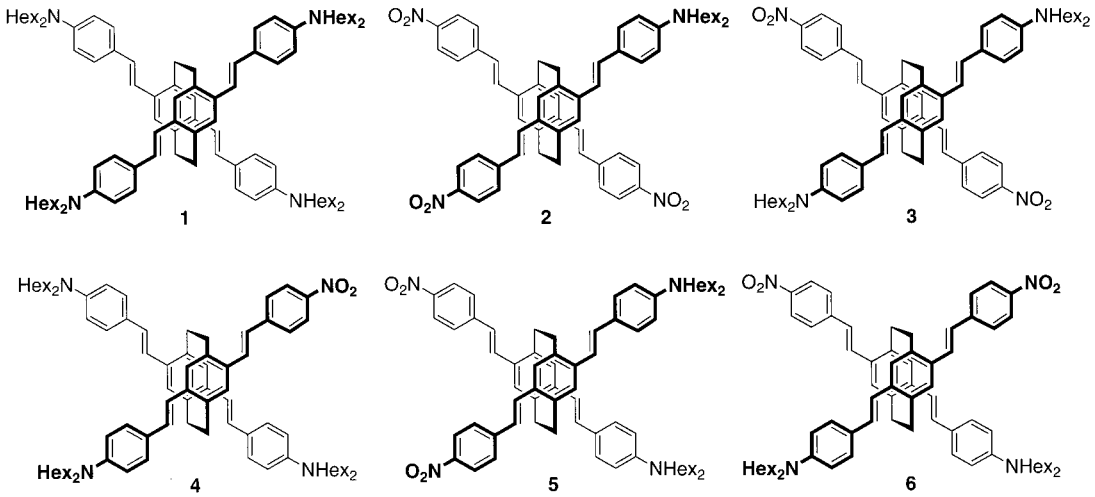

Results and Discussion

Horner−Emmons Precursor for Tetra-Substituted Paracyclophane. Previous experience with tetra-substituted pCp has shown that the palladium-mediated Heck reaction,[22] often used in the formation of phenylenevinylene linkages,[23] results in poor yields and a distribution of partly coupled products. Yields can be as low as 18% when coupling a moderately soluble and reactive vinyl styrene to (4,7,12,15)tetrabromo[2.2]paracyclophane[24] under these conditions, even after careful optimization of solvent, temperature, and reaction time.[17] One concern is that nitrobenzene substitution tends to reduce solubility and would inhibit complete substitution by the Heck route after attachment of one or more of these groups.

To address this challenge, we examined a Horner−Emmons coupling[25] precursor to obtain the desired products, starting with the diethylphosphonatemethyl-substituted paracyclophane precursor. This route has the following advantages: (1) the reaction byproducts are water soluble and enable simpler purification, (2) the phosphonate-substituted pCp is of excellent solubility in typical solvents, and little precipitation of intermediates is expected, and (3) these couplings are typically high yield and produce mainly the *E* isomer.[25]

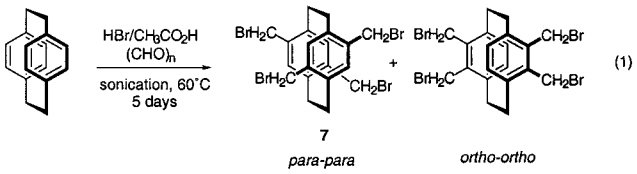

The first synthetic objective was (4,7,12,15)tetra(bromomethyl)-[2.2]paracyclophane (**7**) as the precursor to (4,7,12,15)-tetra-(diethylphosphonatemethyl)[2.2]paracyclophane (**8**). A route to **7** was developed using sonication, instead of stirring, in the bromomethylation of paracyclophane. Paracyclophane and an excess of paraformaldehyde were sealed in a thick-walled Schlenk bomb in a 33% HBr solution in acetic acid and sonicated for 5 days at 60 °C (eq 1). Sonication is thought to counter the low solubility of the paracyclophane starting material. This reaction leads to two isomers, specifically the desired para−para (**7**) and the ortho−ortho ((4,5,12,13)tetra-(bromomethyl)[2.2]paracyclophane). Successive triturations in chloroform give the desired isomer in 20% yield. The (4,7,-12,15)-substitution pattern was confirmed by single-crystal X-ray diffraction (Supporting Information). Crystallographic parameters can be found in Table 1. Compound **7** was readily converted into **8** by heating to 120 °C in triethyl phosphite (eq 2).

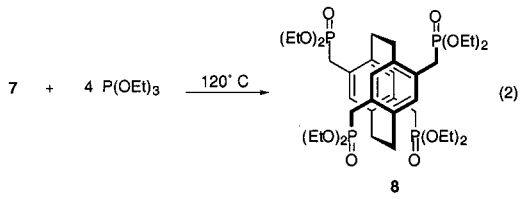

Attempts to use sodium hydride as a base for **8** in THF and DMF were unsuccessful and led to a mixture of products. Sodium ethoxide was equally unsatisfactory. Coupling of 4.2 equiv of 4-dihexylaminobenzaldehyde to **8** using potassium *t*-butoxide as the base leads to 95% yield of **1** after column chromatography of the crude (eq 3). Alternatively, liquid−liquid extraction of the crude followed by successive recrystallizations in hexanes lead to an 86% yield of bright orange cube-shaped crystals that were of sufficient quality for a single-crystal X-ray diffraction experiment. The results of this study are shown in Figure 1. A complete description of the molecular strucure and the crystal lattice can be found in the following section. When compared to alternative protocols, the high yield and purity of the product obtained by Horner−Emmons precursor route are noteworthy.

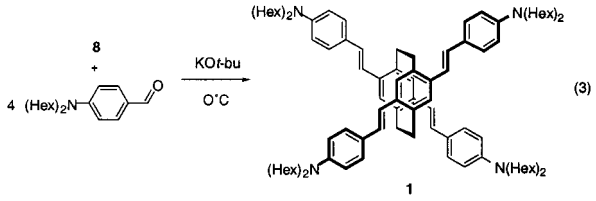

(22) Beletskaya, I. P.; Cheprakov, A. V. *Chem. Rev.* **2000**, *100*, 3009.
(23) (a) Oldham, W. J., Jr.; Lachicotte, R. J.; Bazan, G. C. *J. Am. Chem. Soc.* **1998**, *120*, 2987. (b) Sengupta, S.; Sadhukhan, S. K. *Tetrahedron. Lett.* **1999**, *40*, 9157. (c) Martin, R. E.; Diederich, F. *Angew. Chem., Int. Ed.* **1999**, *38*, 1350.
(24) Reich, H. J.; Cram, D. J. *J. Am. Chem. Soc.* **1969**, *91*, 3534.
(25) Wadsworth, W. S. *Org. React.* **1977**, *25*, 73.

Table 1. Crystal Data and Refinement Parameters for **7**, DD, **1**, and **3**

crystal parameters	**7**	DD	**1**	**3**
chemical formula	$C_{20}H_{20}Br_4$	$C_{46}H_{68}N_2$	$C_{96}H_{140}N_4$	$C_{72}H_{88}N_4O_4$
formula weight	580.00	649.02	1350.12	1073.46
crystal system	triclinic	monoclinic	monoclinic	triclinic
space group (No.)	$P\bar{1}$ (No. 2)	$P21/c$	$C2/c$	$P\bar{1}$ (No. 2)
Z	4	8	4	2
a, Å	8.6099(6)	22.4743(14)	31.858(3)	10.201(3)
b, Å	13.3474(10)	11.6272(7)	16.2284(13)	12.508(4)
c, Å	17.2548(13)	31.793(2)	21.780(2)	24.799(8)
α, deg	101.1140(10)	90	90	101.804
β, deg	97.1880(10)	106.5030(10)	131.1180(10)	97.221(6)
γ, deg	90.1080(10)	90	90	96.463(7)
volume, Å^3	1929.7(2)	7965.7(9)	8483.1(12)	3039(2)
ρ_{calc}, Mg/m^3	1.996	1.082	1.057	1.173
crystal dimens, mm	0.40 × 0.40 × 0.04	0.53 × 0.27 × 0.10	0.53 × 0.40 × 0.13	0.11 × 0.08 × 0.08
temp, K	293	202	202	202
2θ range for data	2−25	2−50	2−50	2−50
total reflections	17 068	68 503	28 312	25 164
independent reflections	6766[Ri(F2) = 0.0512]	14 011[Ri(F2) = 0.0709]	5204[Ri(F2) = 0.0718]	10 609[Ri(F2) = 0.0862]
no. obsd data	6755 ($I > 2\_(I)$)	14 011 ($I > 2\_(I)$)	5163 ($I > 2\_(I)$)	10 601 ($I > 2\_(I)$)
no. parameters varied	433	873	512	725
μ, mm^{-1}	8.341	0.061	0.060	0.072
$R_1(F)$, w$R_2(F^2)$, ($I > 2\sigma(I)$)	0.0709, 0.1561	0.0428, 0.1002	0.1037, 0.2375	0.0759, 0.1619
$R_1(F)$, w$R_2(F^2)$, all data	0.1094, 0.1649	0.1136, 0.1259	0.1650, 0.2678	0.1934, 0.1859
GOF on F^2	1.498	0.842	2.343	1.055

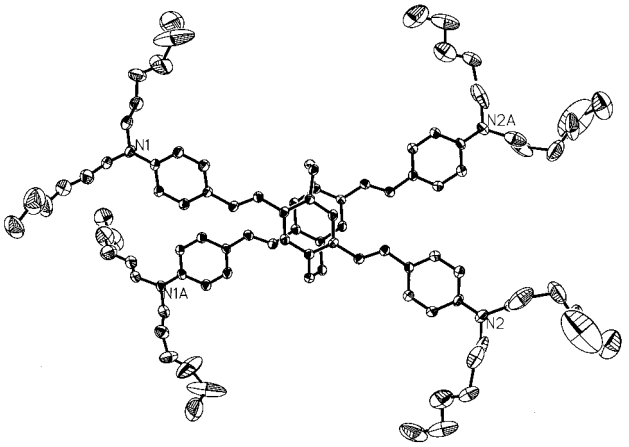

Figure 1. ORTEP drawing of **1**. Ellipsoids are shown at 20% probability, and hydrogens are omitted for clarity.

Compound **2**, a less symmetric target, was obtained by stepwise addition of 1 equiv of potassium *t*-butoxide and 4-dihexylaminobenzaldehyde to **8** followed 24 h later by excess 4-nitrobenzaldehyde and 3 equiv of potassium *t*-butoxide (eq 4). Purification was achieved by HPLC separation performed on a nitro-derivatized silica column providing a 68% yield. The best results are obtained for this separation using a gradient of chloroform in hexanes.

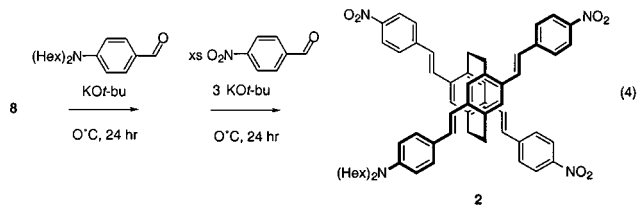

The simultaneous synthesis of the three regioisomers of two-donor/two-acceptor coupling, specifically **3**, **5**, and **6**, was attempted starting with **8**. Two equivalents of 4-dihexylaminobenzaldehyde were coupled to **8** with potassium *t*-butoxide in DMF (eq 5).

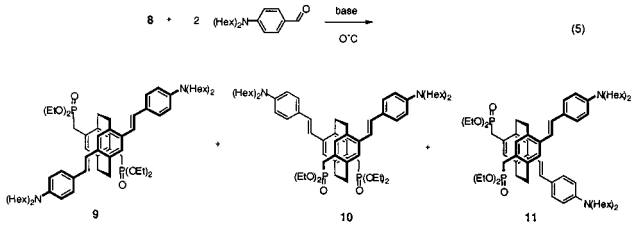

The reaction in eq 5 was analyzed by HPLC using a nitro-derivatized silica column. Small amounts of **1** and several unidentified products were formed in this reaction along with one major fraction (68% yield with respect to **8** after HPLC separation). NMR spectroscopy and mass spectrometry (MS) of this fraction were consistent with a two-donor coupled product. MS offered further insight into the absolute configuration of this single regioisomer. Fragmentation of pCp under mild electron ionization (EI) conditions shows predominately *p*-xylylene ion radicals.[26] A large ion peak at $m/z = 673$ was observed that is consistent with the two-donor coupled *p*-xylylene ion. These data led to the assignment of the major fraction from DMF as (4,7)bis(diethylphosphonatemethyl)-(12,-15)bis(4′-dihexylaminostyryl)[2.2]paracyclophane (**9**). Further reaction with an excess of 4-nitrobenzaldehyde and potassium *t*-butoxide leads to 84% yield of **3** (eq 6). The substitution assigned was fully confirmed by a single-crystal X-ray diffraction study of **3** (Figure 2).

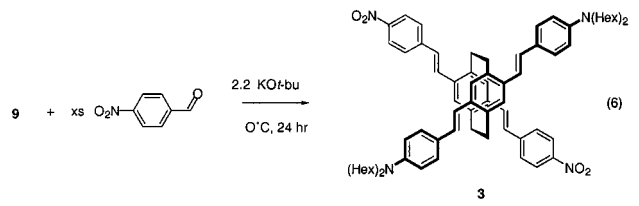

The two-donor coupling to **8** in the less polar solvent THF resulted in two fractions by HPLC, which could be confirmed

(26) Reich, H. J.; Cram, D. J. *J. Am. Chem. Soc.* **1969**, *91*, 3534.

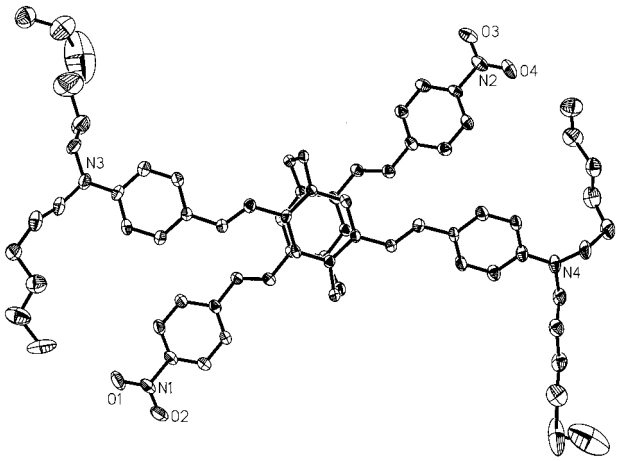

Figure 2. ORTEP drawing of **3**. Ellipsoids are shown at 30% probability, and hydrogens are omitted for clarity.

Scheme 3

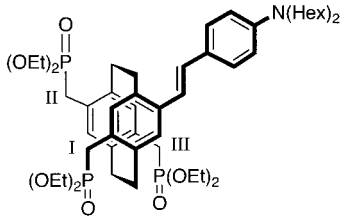

as two-donor coupling products by MS. The first fraction was **9** in 23% yield. Examination of the fragmentation of the second fraction showed a large ion peak at $m/z = 540$ which would be consistent with the structure of (4,12)bis(diethylphosphonatemethyl)-(7,15)bis(4′-dihexylaminostyryl)[2.2]paracyclophane (**10**, in eq 5) or (4,17)bis(diethylphosphonatemethyl)-(7,12)bis(4′-dihexylaminostyryl)[2.2]paracyclophane (**11**), where each pCp ring is substituted with one donor styrene and a benzyl diethylphosphonate. Results from a ^{1}H NMR COSY experiment for the second fraction were consistent with the structure shown for **10** (see Supporting Information). Further reaction of **10** with 4-nitrobenzaldehyde and potassium *t*-butoxide afforded **6**. Interestingly, no fraction in either the DMF or the THF reaction was found to correspond with **11**.

To further investigate the regioselectivity of **8** toward two-donor coupling, quantitative analytical HPLC was performed for this reaction in both DMF and THF using samples of **9** and **10** as external standards. As solvent polarity increases (i.e., DMF), selectivity for **9** increases (68% and 10% of **9** and **10**, respectively), while reducing polarity (THF) leads to **10** as the major product (23% and 57% of **9** and **10**, respectively). In an attempt to understand the factors at work in this selectivity, consider a situation in which the first coupling of donor benzaldehyde is complete and the product distribution of the reaction is determined solely by the second coupling step. The three remaining reaction sites are shown and labeled in Scheme 3. Site III is ruled out on the basis of steric interference from the dihexylaminostyryl group. Formation of **11** is thus not observed. In the more polar solvent DMF, reaction at site I is preferred, leading to the formation of **10**. In THF, reaction at site II is considerably enhanced, while site I remains somewhat active. It is not clear whether this reversal in selectivity is due to different kinetic preferences in the deprotonation step or to differences in reactivity of the carbanion toward the aldehyde. The latter condition would require carbanion exchange/equilibration during the time scale of the reaction. Regardless of the exact origin of the observed selectivity, this system reflects a unique interplay of factors that allows for regiochemical control by choice of reaction solvent.

Compound **4**, with three 4-dihexylaminostyryl and one 4-nitrostyryl group, was not obtained from the tetraphosphonate precursor by successive couplings in a manner similar to **2**. HPLC analysis of attempts to couple 1 equiv of nitrobenzaldehyde to **8** in both THF and DMF revealed a broad distribution of partially coupled products. Attempts to first couple 3 equiv of dihexylaminobenzaldehyde invariably lead to a distribution of intermediates along with a substantial amount of **1**.

Bromo/Formyl Combinations for Site-Specific Coupling. Limitations to the use of **8** for the synthesis of **4** and **5** lead us to search for a complimentary tetrasubstitution precursor. Monolithiation of (4,7,12,15)tetrabromo-[2.2]paracyclophane[27] (**12**) followed by DMF quenching yields [4,7,12]tribromo-15-formyl[2.2]paracyclophane (**13**) (eq 7). Flash chromatography on silica support provided purification of the product for a yield of 37%. The NMR and MS spectra were consistent with the proposed structure, and fragmentation under EI conditions for MS showed ions that are consistent with both a dibromo and bromo-formyl substituted *p*-xylylene radicals ($m/z = 262$ and 210, respectively).

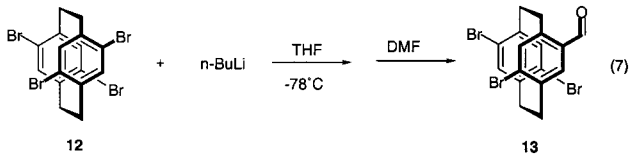

Compound **13** was then subjected to Heck coupling with 6 equiv of 4-dihexylaminostyrene. The reaction mixture was separated using flash chromatography resulting in a 64% yield of the desired (4,7,12)tris(4′-dihexylaminostryl)-15-formyl[2.2]-paracyclophane (**14**) (eq 8).

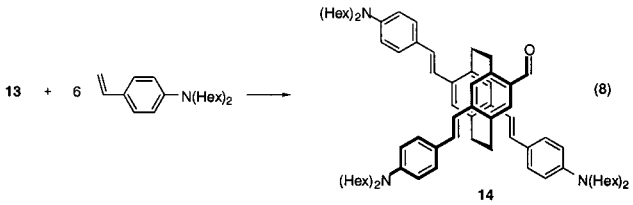

Compound **14** was then subjected to a Horner−Emmons coupling with 4-nitrophenylmethanephosphonate using potassium *t*-butoxide as base (eq 9). Again, this reaction could be purified by flash chromatography for a yield of 81% for this step.

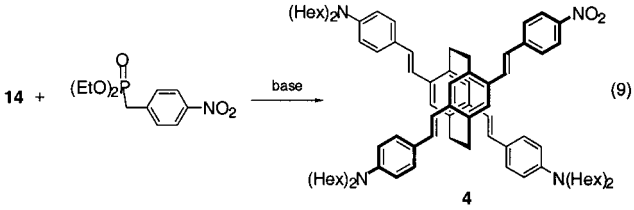

(27) Reich, H. J.; Cram, D. J. *J. Am. Chem. Soc.* **1969**, *91*, 3527.

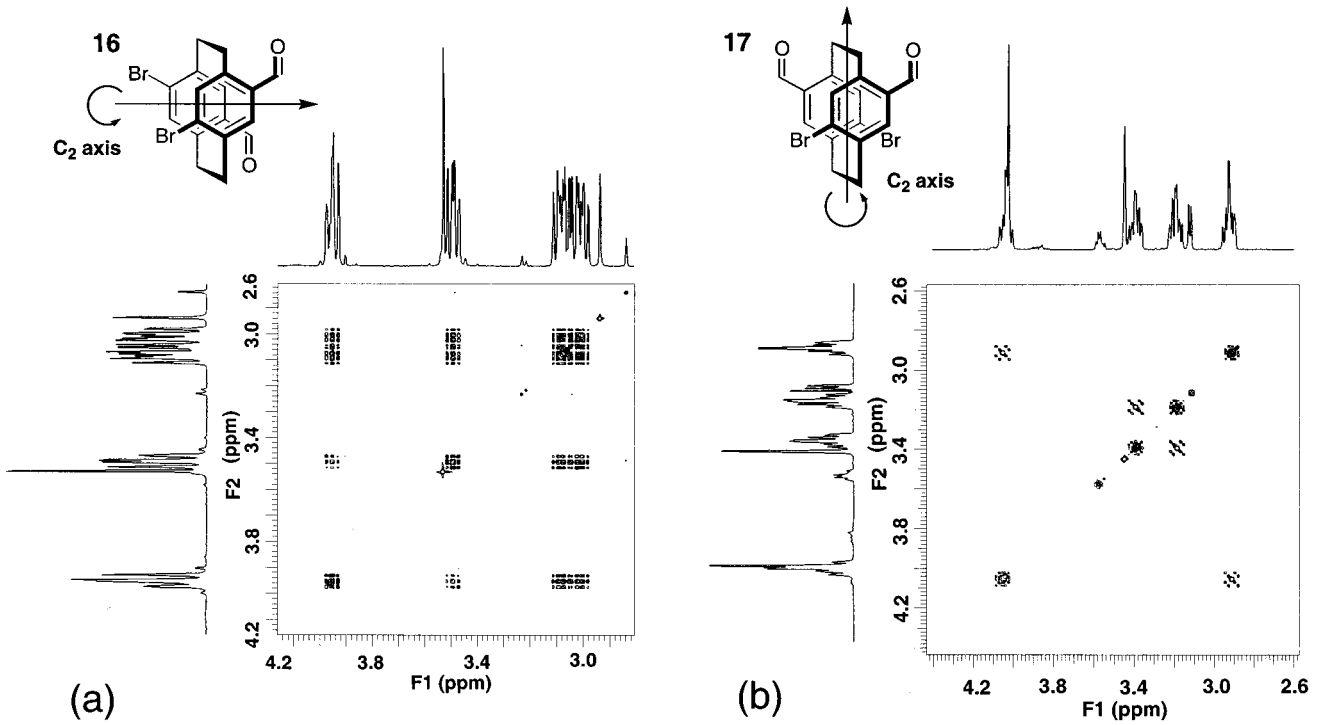

Figure 3. A comparison of 2D-COSY proton spectra for compounds (a) **16** and (b) **17**. The methylene regions of both COSY spectra which contain resonances for the protons bound to the paracyclophane bridging carbons are displayed.

A similar approach was used to obtain **5** and **6**. Compound **12** was treated with 2 equiv of *n*-BuLi followed by quenching with DMF (eq 10). Surprisingly, only two isomers were obtained. The fragmentation of these isomers under EI during MS gave evidence that the two isomers obtained were 4,15-dibromo-7,12-diformyl[2.2]paracyclophane (**16**) and 4,12-dibromo-7,15-diformyl[2.2]paracyclophane (**17**). The mass spectrum of **15** would contain major ion peaks at $m/z = 160$ and 262, neither of which were observed for the two products. Instead, large peaks at $m/z = 210$ corresponding to the bromoformyl-*p*-xylylene radical ion were recorded in the mass spectra of the two products. The absence of **15** would be consistent with the higher energy associated with two negative charges created by dilithiation on a single benzene ring relative to one charge on each ring of paracyclophane to yield **16** and **17**. These two isomers could be further differentiated by 2-dimensional ^{1}H NMR spectroscopy. Specifically, the C_2 axis of symmetry lies differently in both isomers with respect to the bridging protons. For **16**, the four protons on a single ethylene bridge are inequivalent; therefore the COSY spectrum in Figure 3a shows correlation between all the bridging protons. In the case of **17**, due to the orientation of the C_2 axis, there are only two inequivalent protons on a single arm. As shown in Figure 3b, this relationship results in a much simpler 2-D spectrum. The yields for **16** and **17** were 55% and 34%, respectively.

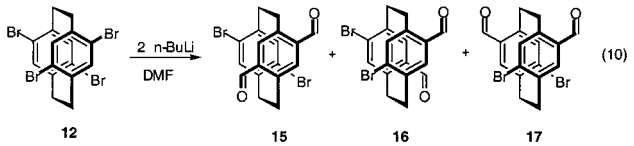

Compounds **16** and **17** were both subjected to Heck coupling with the donor styrene followed by a Horner−Emmons coupling with the phosphonate precursor for the nitrostyryl group to yield **5** and **6**, respectively. For example, the reaction of **16** with excess 4-dihexylaminostyrene under Heck conditions for 24 h leads to a 93% yield of (7,12)-diformyl-(4,15)-(4′-dihexylaminostyryl)-[2.2]paracyclophane (**18**) after flash chromatography (eq 11).

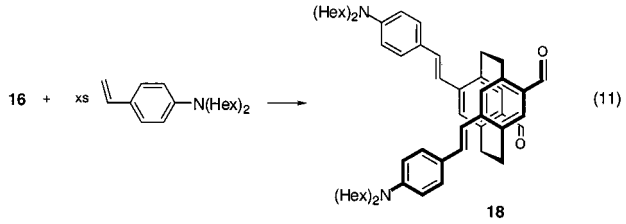

The final step in the synthesis of **5** requires coupling of **18** to 4-nitrophenylmethanephosphonate with potassium *t*-butoxide as base in THF for a 79% yield (eq 12). Performing the reactions shown in eqs 11 and 12, but starting with **17**, provides access to compound **6**.

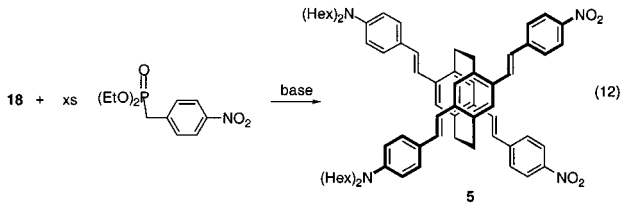

Synthesis of 1-(4′-Dihexylaminostyryl)-4-(4′′-nitrostryl)-benzene (DA), 1,4-Di(4′-nitrostyryl)benzene (AA), and 1,4-Bis(4′dihexylaminostyryl)benzene (DD). The parent chromophores were synthesized according to previously reported procedures.[28−30] For example, DD was prepared by a coupling of 2 equiv of 4-dihexylaminobenzaldehyde with α,α′-diphosphonate-*p*-xylene. The synthesis of DA consisted of a stepwise coupling of 1 equiv of dihexylaminobenzaldehyde with α,α′-

diphosphonate-*p*-xylene, followed by 1 equiv of 4-nitrobenzaldehyde. The crystal structure of DD was obtained from a crystal grown from hexanes (Supporting Information). Crystallographic parameters can be found in Table 1, and a full description of the molecule and the lattice is found in the following section.

Crystallographic Packing Features. We have previously reported the crystal structure and lattice properties of a wide variety of distyrylbenzene derivatives.[31,32] In this section, we present structural data for "dimerized" chromophores **1** and **3** and compare the arrangement of molecules in the lattice against the parent structures DD and AA. The "pairing" of chromophores into a single pCp molecule creates a unique situation in which the basic unit of the packing unit has been constrained by covalent attachment. The features that are of greatest interest are those that reflect the disposition of the conjugated distyrylbenzene fragments relative to one another; thus we omit a detailed description of the exact arrangement of aliphatic solubilizing groups.

Intramolecular metrical parameters are normal for the DD molecular structure, and the terminal rings deviate from planarity with the central ring by ∼25°.[33] The molecules stack at an oblique angle, and neighboring stacks are oriented such that the long axes of the molecules in neighboring stacks are roughly perpendicular. This orientation leads to a criss-cross appearance to the phenylenevinylene portion of the chromophore when viewed along the *a*-axis (Figure 4). In this view of the lattice, the hexyl chains are omitted. With this view, a layered structure is revealed alternating between the distyrylbenzene portion of the chromophore and the hexyl groups. Although no conspicuous close contacts are present, the formation of layers between the phenylenevinylene and alkyl regions reflects an advantage to separation over a structure where they are more continuous.

The structure and lattice of AA·**2** DMF has been described previously[31] and will be covered only briefly here. One of the most characteristic features of this structure is the overlapping nitrostryl subunits of the molecule, where the NO_2 group is adjacent to the olefin of its neighbor. This overlap for AA·**2** DMF leads to a bricklike structure that forms channels in which the two DMF molecules are situated.

Single cube-shaped crystals of **1** were grown from hexanes. The methylene bridge of the pCp core is twisted with a torsion angle for the ethyl bridge of 25.24(3)°. There is a crystallographically imposed C_2 axis, with the terminal rings deflected from planarity from the central ring by ∼10° and ∼14°. This difference is a consequence of inequivalent environments for the two ends of the parent chromophore due to the orientation of one enantiomer relative to the other. In comparison with the conformation suggested in Scheme 2, the actual structure features the twisted core accompanied by a 180° rotation of the pCp−olefin bond. This change brings the long axis of the bound parent chromophores closer to a parallel arrangement than the proposed structure.

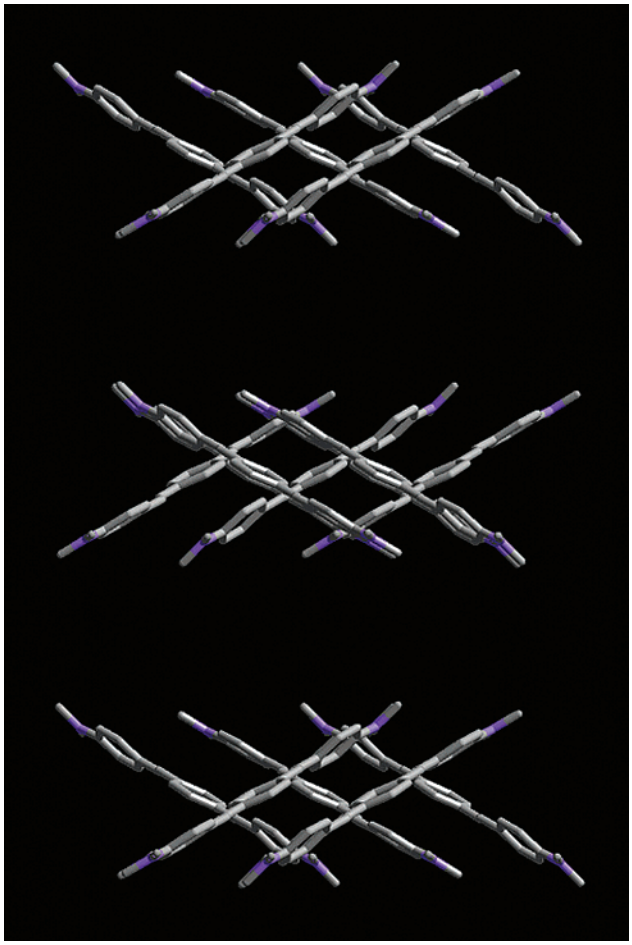

Figure 4. Packing diagram of DD viewed down the *a*-axis. The hexyl carbons are not shown for clarity.

The molecules of **1** are arranged in the lattice within "interlocking" columns that run along the *b*-axis with the terminal hexyl groups intertwined in a complex fashion. Molecules in any one column are a single enantiomer with the other enantiomer located in the closely neighboring column. Figure 5 shows a view along the *c*-axis that features a superposition of the enantiomeric columns. With this view, a layered structure appears with interlocking chromophore regions where the hexyl groups fill the void between layers.

Deep red crystals of **3** suitable for X-ray diffraction were grown from acetone. Figure 6a shows the enantiomeric pair without the hexyl groups for clarity. Again the pCp-based compound displays a twisted core and an alignment of the two parent chromophores closer to a parallel arrangement that one might initially expect. Deviations from planarity for the styryl groups relative to the central ring to which they are attached are much more complex than those in **1**. Angles range from 2.476(4)° for one nitrostyryl group to 28.578(4)° for the dihexylaminostryl on the opposing face. Overall, these deviations follow the pattern seen in **1** where styryl groups on one face are more distorted than the other (2.476(4)° and 7.687(4)° for one face, 28.578(4)° and 19.255(4)° for the other).

Further inspection of Figure 6a shows a reciprocal overlap of nitro groups with the neighbor's olefin groups, a configuration

(28) Wadsworth, D. H.; Schupp, O. E.; Seus, E. J., Ford, J. A., Jr. *J. Org. Chem.* **1964**, *30*, 680.
(29) Nakatsuji, S.; Matsuda, K.; Uesugi, Y.; Nakashima, K.; Akiyama, S.; Katzer, G.; Fabian, W. *J. Chem. Soc., Perkin Trans. 2* **1991**, *6*, 861.
(30) Rumi, M.; Ehrlich, J. E.; Heikal, A. A.; Perry, J. W.; Barlow, S.; Hu, Z.; McCord-Maughon, D.; Parker, T. C.; Röckel, H.; Thayumanavan, S.; Marder, S. R.; Beljonne, D.; Brédas, J.-L. *J. Am. Chem. Soc.* **2000**, *122*, 9500.
(31) Bartholomew, G. P.; Bazan, G. C.; Bu, X.; Lachicotte, R. J. *Chem. Mater.* **2000**, *12*, 1422.
(32) (a) Wu, G.; Jacobs, S.; Lenstra, A. T. H.; Van Alsenoy, C.; Geise, H. J. *J. Comput. Chem.* **1996**, *17*, 1820. (b) Van Hutton, P. F.; Wildeman, J.; Meetsma, A.; Hadziioannou, G. *J. Am. Chem. Soc.* **1999**, *121*, 5910.
(33) Torsional distortions in stilbenoid compounds are characterized by a relatively flat potential energy surface, see: Hoekstra, A.; Meertins, P.; Vos, A. *Acta Crystallogr.* **1975**, *B31*, 2813.

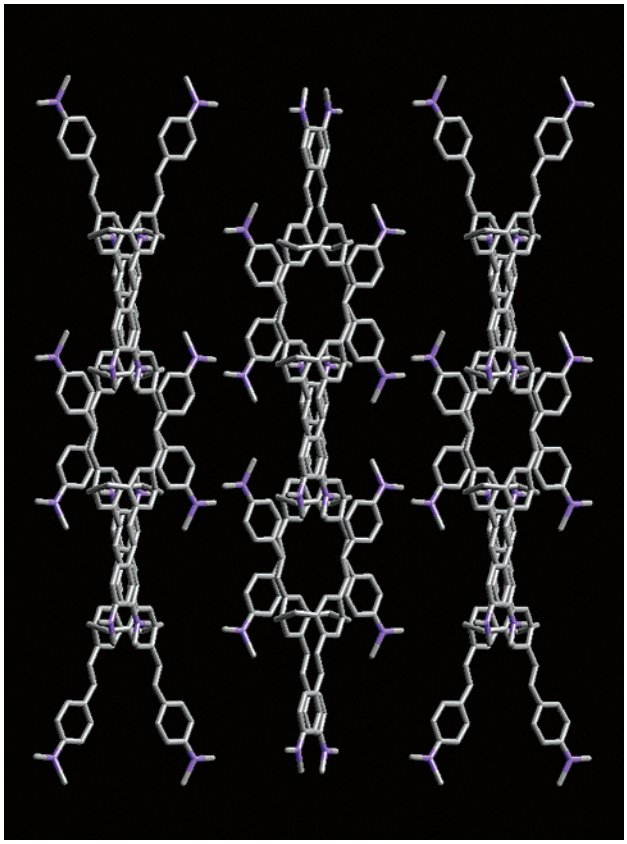

Figure 5. Packing diagram from the crystal structure of **1** viewed along the *c*-axis demonstrating the segregation of the distyrylbenzene portions from the alkyl regions in an interlocking layered strucure. The hexyl groups are not shown for clarity.

seen in the parent AA. Figure 6b shows the lattice with a view along the *c*-axis and reveals the dihexylaminostyryl groups opposite each other. The nitrostyryl interactions along the *a*-axis and the end-to-end packing of the dihexylaminostyryl groups running along the *b*-axis result in channels that propagate along the *c*-axis. These channels are, in fact, where the alkyl groups are contained. In essence, chains of overlapped constituent AA chromophores "cross-link" the segregated layers formed by end-to-end interactions among the DD portion of **3**. After pairing of the two parent chromophores, elements of their individual packings appear to coexist. The high level of distortion within the individual molecules of **3** in this lattice may reflect the competition of these packing motifs.

Optical Spectroscopy. To provide a baseline measure of the changes in the optical spectroscopy of **1**−**6**, the absorption and emission spectra of DD, AA, and DA are presented first. Figure 7 contains the spectra of DD in hexanes and AA in $CHCl_3$. The absorption λ_{max} of DD is ∼400 nm, and the emission maximum occurs at 437 nm. The spectroscopy of this molecule is characterized by structured emission with a normal Stokes shift. Because of the poor solubility of AA in hexanes, the solution spectra were collected in chloroform. In $CHCl_3$, AA exhibits an absorption maxima at 400 nm, while $\lambda_{max(em)} = 535$ nm, a 135 nm Stokes shift. Spectroscopic data for AA in dioxane have been reported previously[34] and showed an absorption maxima at 395 nm and $\lambda_{max(em)} = 415$ nm. This is a considerably smaller Stokes shift (20 nm) relative to the data from $CHCl_3$ (135 nm). The absorption spectra of DA in hexanes are characterized by two strong absorption bands (Figure 8) with $\lambda_{max} = 433$ nm and a smaller band at 330 nm. The emission spectrum is structured and has a maximum at 530 nm.

Figure 9 shows the emission and absorption spectra for **1** in hexanes and $CHCl_3$. Emission in hexanes is structured and exhibits a relatively small Stokes shift ($\lambda_{max(abs)} = 431$ nm, $\lambda_{max(em)} = 477$ nm). In $CHCl_3$, the structure in the emission is lost, and the Stokes shift increases ($\lambda_{max(abs)} = 440$ nm, $\lambda_{max(em)} = 560$ nm). This solvatochromatic shift is consistent with an excited state that is more polarized than the ground state. The excitation spectra in both solvents match the absorption spectra. Note that the absorption maximum in hexanes is red-shifted by 30 nm relative to DD. This extended conjugation due to the pCp junction has been observed in similar "criss-cross" delocalized pCp chromophores.[17]

Figure 10 contains the absorption and emission of **5** and **6** in hexanes. These two chromophores correspond to regioisomers of DA dimerization via pCp. The first thing to note is the red-shift in absorption for these compounds relative to DA. The absorption maxima for **5** and **6** are 470 and 460 nm, respectively, which contrast to the maximum for DA at 433 nm. Cofacial overlap of the central rings of the parent chromophores leads to extended conjugation and additional charge transfer from donor and acceptor combinations across the pCp bridge. The red-shift for the absorption and emission of **5** relative to **6** is of additional interest. This difference is likely a result of a greater stabilization of the charge redistribution by the dipole orientations of the "parent" chromophores. The dipoles of the parent chromophores should result in a larger net dipole for the arrangement found in **5** relative to **6**.

Spectra for **3**, the pairing of DD with an AA chromophore, are presented in Figure 11. The maximum for absorption in hexanes occurs at 417 nm, with a weak and broad tail in the 475−600 nm region. Emission from hexanes shows *two* bands. One is centered at approximately 500 nm, while the maximum of the more intense band appears around 690 nm. The ratio of the two bands does not depend on sample history. In $CHCl_3$, there *appears* to be a *blue*-shift in the emission (∼600 nm), while absorption is slightly red-shifted (440 nm). The overall fluorescence quantum efficiency is low; in hexanes it is 0.5 ± 0.3% and in chloroform 3 ± 2%.

Emission spectra, exciting at 420 nm, in different ratios of hexanes and $CHCl_3$ with a constant concentration of **3** were collected (for spectra see Supporting Information). At 20% $CHCl_3$, the band at 690 nm in hexanes is essentially quenched, while the 500 nm band remains. This higher energy band appears to gradually red-shift as the concentration of $CHCl_3$ is increased to 50%. The integrated intensity of the band at ∼600 nm in 100% $CHCl_3$ rivals that of the 690 nm band in hexanes. These data show that the band in chloroform is a normal solvatochromic shift of the band at ∼500 nm in hexanes.

Excitation spectra observing at different emission wavelengths in both hexanes and $CHCl_3$ were collected. Observing fluorescence at 690 nm, we see the absorption spectrum reproduced in the excitation spectrum. Observing at 520 nm, the excitation spectrum no longer exhibits the beginning of the 475−600 nm tail. The absence of this tail in the excitation spectrum in $CHCl_3$, observing at 600 nm, reveals a common origin for both the band

(34) Nakatsuji, S.; Matsuda, K.; Uesugi, Y.; Nakashima, K.; Akiyama, S.; Katzer, G.; Fabian, W. *J. Chem. Soc., Perkin Trans. 2* **1991**, *6*, 861.

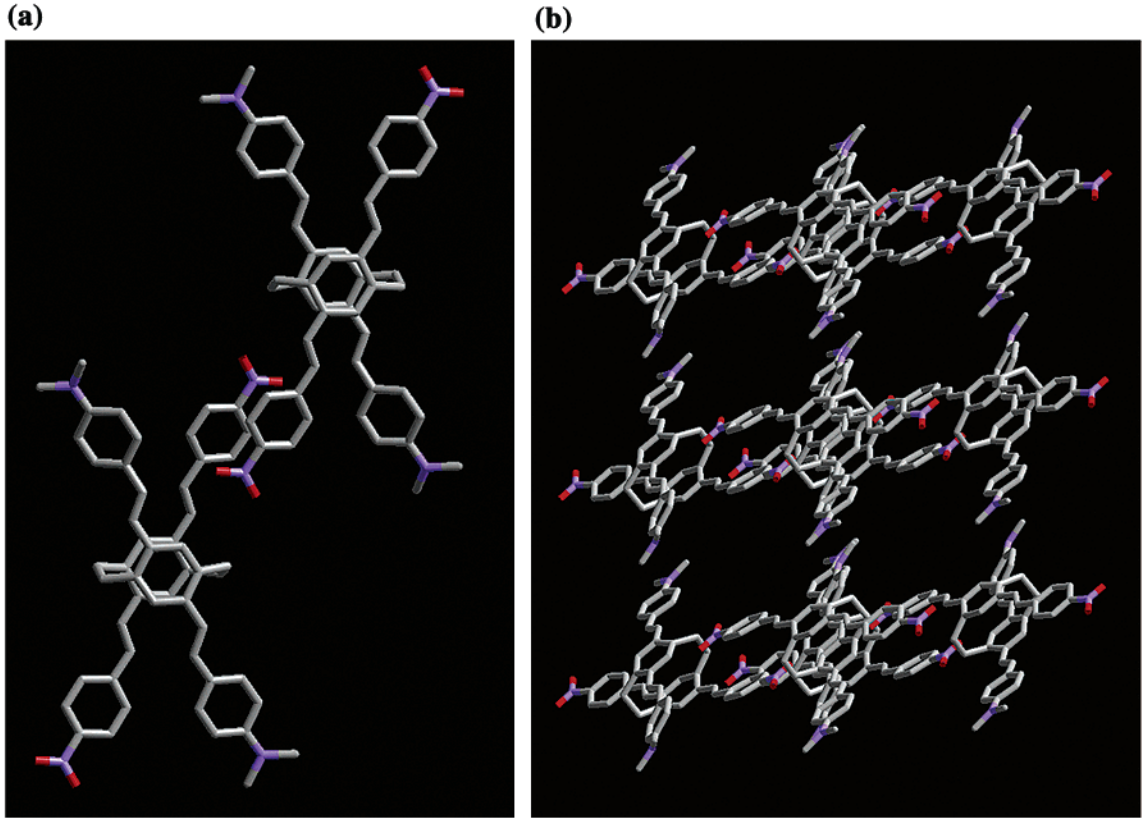

Figure 6. The enatiomeric pair of molecules (a) and packing diagram (b) from the crystal structure of **3** viewed along the *c*-axis. Note the overlapping nitrostyryl groups. The long molecular axis of the dihexylamino-substituted portion of **3** is parallel to the *b*-axis, while the long axis of the nitro-derivatized portion runs parallel to the *a*-axis. The hexyl groups, which are not shown for reasons of clarity, are contained in the channels that run parallel to the *c*-axis.

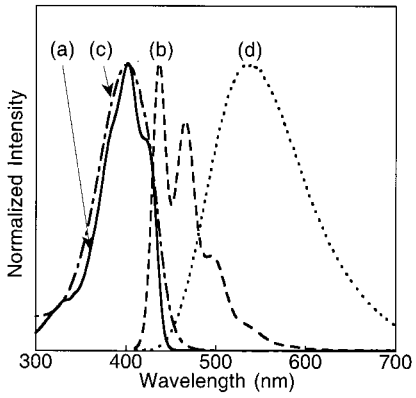

Figure 7. Normalized absorption (a) and emission (b) (exciting at 380 nm) of DD in hexanes and absorption (c) and emission (d) (exciting at 400 nm) of AA in $CHCl_3$.

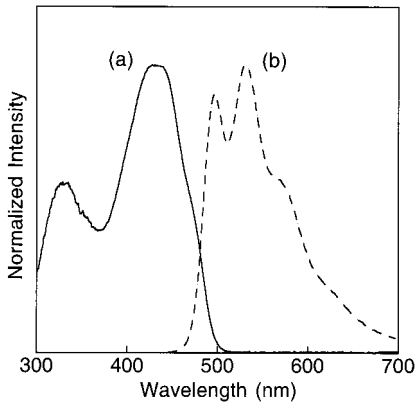

Figure 8. Normalized absorption (a) and emission (b), exciting at 433 nm, of DA in hexanes.

at 500 nm in hexanes and the ~600 nm band in $CHCl_3$. All of these experiments were performed using material that showed a single peak by analytical HPLC using different solvent combinations.[35]

The fact that two bands are observed indicates that the emission at 500 nm is from the second excited state (S_2). The overall efficiency of this process is low, in the order of 0.05%. Emission at 690 nm is likely from a lower-lying ICT state (S_1).[36] As solvent polarity is increased, the polar ICT excited state is quenched, and the remaining emission results from $S_2 \rightarrow$ ground-state relaxation. The observed participation in hexanes of S_2 in the emission from S_1 indicates that the rates of fluorescence decay and internal conversion to S_1 are within the same order of magnitude and thus competitive.

To account for the spectroscopy of **3**, we propose the excitation process outlined in Scheme 4. The oscillator strength for S_1 excitation is considerably smaller than the S_2 counterpart. After excitation to S_2, the molecule may relax to S_1 or decay by radiative and nonradiative paths directly from S_2. The partition of the two processes depends on the ratio of the sum total of the rates of fluorescence from S_2 (k_{F2}) and nonradiative relaxation from S_2 (k_{NR2}) (excluding internal conversion to S_1) to the rate of internal conversion to S_1 (k_{IC}). The magnitude of

(35) Two emission bands are also observed by single molecule spectroscopy. (a) Sommers, M.; Bartholomew, G. P.; Buratto, S. K.; Bazan, G. C., work in progress. (b) Mason, M. D.; Sirbuly, D. H.; Carson, P. J.; Buratto, S. K. *J. Chem. Phys.* **2001**, *114*, 8119.

(36) Quantum mechanical calculations show substantial charge-transfer character to the S_1 state: Ottonelli, M.; Mukamel, S., work in progress.

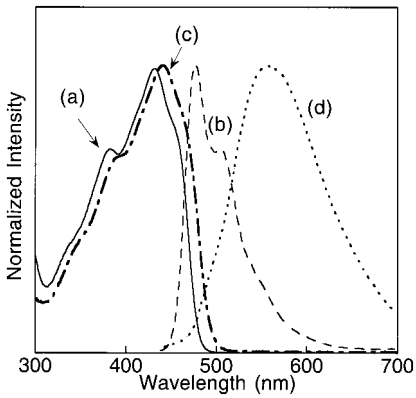

Figure 9. Normalized absorption (a) and emission (b) of **1** in hexanes and absorption (c) and emission (d) in $CHCl_3$. Both emission scans were collected exciting at 420 nm.

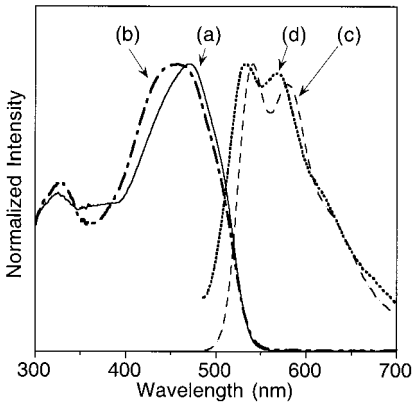

Figure 10. Normalized absorption of **5** (a) and **6** (b) and emission of **5** (c) and **6** (d) in hexanes. Emission data were both collected exciting at 460 nm.

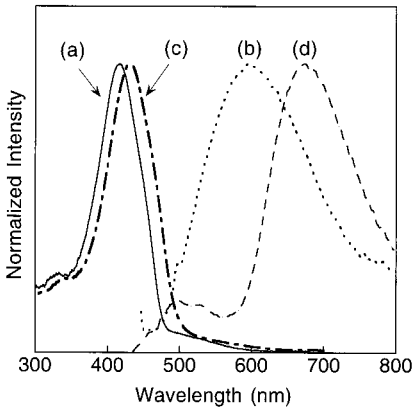

Figure 11. Normalized absorption (a) and emission (b), exciting at 417 nm, of **3** in hexanes and absorption (c) and emission (d), exciting at 431 nm, in $CHCl_3$.

these rates, in addition to the ratios of k_{F2}/k_{NR2} and k_{F1}/k_{NR1} in hexanes, is such that emission from S_1 and S_2 is observed. That emission from S_2 occurs is an interesting violation of Kasha's rule.[37] In $CHCl_3$, emission from S_1 is quenched, and only the residual S_2 fluorescence is observed.

The absorption, emission, and excitation spectra of **2** in hexanes are presented in Figure 12. Compound **2** represents the pairing of a DA chromophore with the symmetric acceptor

(37) Klessinger, M.; Michl, J. *Excited States and Photochemistry of Organic Molecules*; VCH Publishers: New York, 1995.

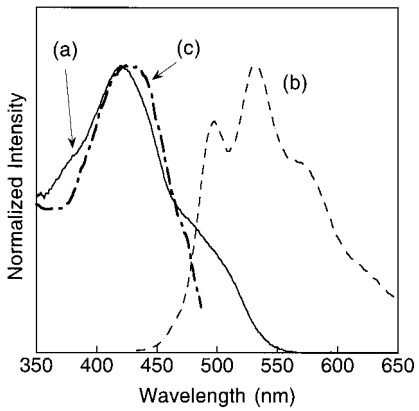

Figure 12. Normalized absorption (a), emission (b), and excitation (c) of **2** in hexanes. Emission data were collected exciting at 419 nm, and the excitation was monitored at 530 nm.

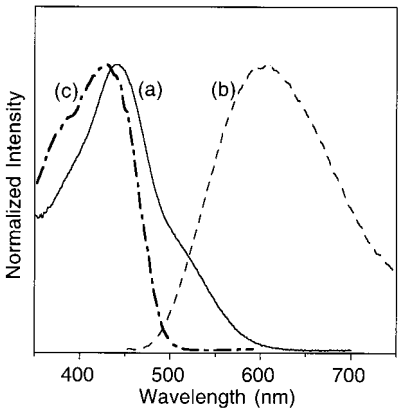

Figure 13. Normalized absorption (a), emission (b), and excitation (c) of **2** in $CHCl_3$. Emission data were collected exciting at 440 nm, and the excitation was monitored at 605 nm.

Scheme 4

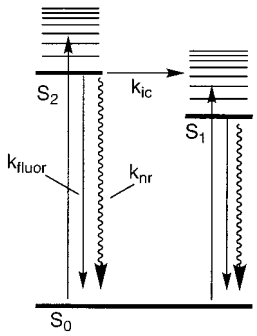

parent, AA. The most notable feature is the penetration of the absorption band well into the emission band. Specifically, the emission band begins at ~450 nm, while emission trails well past 550 nm. The excitation spectrum of **2** indicates that the broad shoulder in the absorption spectrum, located roughly in the 475−550 nm region, does not give rise to emission. The emission from hexanes is structured. Emission from $CHCl_3$ is red-shifted to ~600 nm, and the structure is lost (Figure 13).[4] Again the low energy shoulder region is missing in the excitation spectrum observed at $\lambda_{max(em)}$.

The absorption, emission, and excitation spectra of **4**, the combination of DA with DD, are similar to those of **2** and are presented in Figure 14. Note again the penetration of the absorption shoulder well into the emission band in hexanes, as well as the absence of that shoulder in the excitation spectrum.

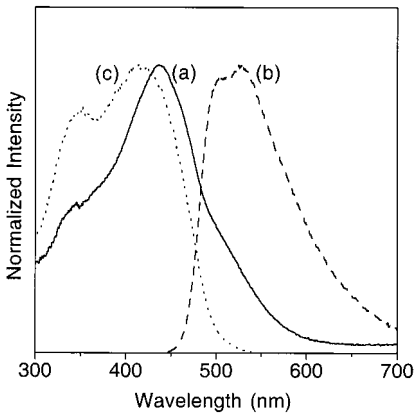

Figure 14. Normalized absorption (a), emission (b), and excitation (c) of **4** in $CHCl_3$. Emission data were collected exciting at 437 nm, and the excitation was monitored at 550 nm.

Scheme 4 can also be used to account for the photophysics of **2** and **4**. Molecule **2** will be used to guide discussion. Excitation in the region of 400−450 nm for **2** promotes the molecule to S_2. The low energy "shoulder" seen in the absorption corresponds to S_1 excitation. Nonradiative relaxation dominates from S_1, that is, $k_{F1} \ll k_{NR1}$, and this is not an emissive state. All of the emission thus originates from S_2, and $k_{F2} + k_{NR2}$ are competitive (at least within 2 orders of magnitude) with k_{IC}.

Conclusion

In summary, the synthetic methodology to prepare molecules **1**−**6** is presented. These molecules correspond to the possible regioisomers that result from bringing together distyrylbenzene chromophores[38] containing donor and acceptor groups across the pCp bridge. The tetraphosphonate precursor **8** is a key intermediate because of its versatility in generating molecules **1**−**3**, and because it enables coupling with Horner−Emmons procedures, which are of higher yields and easier to purify than Heck protocols. For the preparation of **4**, use of the monoformyl tribromide derivative **13** is required. In the case of the orientational isomers **5** and **6**, we rely on 2-fold bromo-lithium exchange, as shown in eq 10, which provides the requisite **16** and **17** precursors. The only missing combination of the series, corresponding to four dinitrostyryl groups on pCp, is not obtained because of its intrinsic low solubility in common organic solvents.

By constraining the distance and orientation of two distyrylbenzene chromophores by pCp, one observes lattice arrangements different from those of the parent chromophores. The principal reason is the intrinsic chirality of the dimers. Many of the original crystal engineering "synthons" remain.[39] In particular, the alignment of electron-deficient nitro fragments which prefer to rest adjacent to polarizable olefin groups is retained. Additionally, the distrylbenzene chromophore portion of these molecules readily segregates from the alkyl solubilizing side groups, even in the presence of additional interchromophore interactions and constraints. These guiding principles may prove useful in the design of organic solids with optimized interchromophore delocalization and/or bulk ordering.

The disposition of donor and acceptor groups within the three-dimensional conjugated fragment provided by the tetrastyryl-pCp fragment gives rise to unexpected optical properties. For **1**, **5**, and **6**, additional delocalization occurs, as expected on the basis of previous work on through-space delocalized paracyclophane molecules. However, in the case of **2**, **3**, and **4**, the relaxation from S_2 to S_1 by internal conversion is not complete, and emission from S_2 can be observed. Interestingly for **3** in hexanes one observes emission from S_2 and S_1. Changing solvents from hexanes to chloroform results in quenching from S_1, and the result is an anomalous blue-shift in emission by switching to the more polar solvent. Scheme 4 can be used to provide a simplified picture for these processes. Molecules **2** and **4** operate similarly; however, no emission from S_1 has been observed under our experimental conditions.

Experimental Section

General Details. All synthetic manipulations were performed under an inert atmosphere in a nitrogen filled glovebox or using Schlenk techniques. All reagents were obtained from Aldrich and were used as received. ^{1}H NMR spectra were obtained using a Varian Unity 400 MHz spectrometer. ^{13}C NMR and 2D-^{1}H COSY spectra were obtained using a Varian Unity INOVA 500 MHz spectrometer. High-resolution mass spectra were performed on a VG-70SE double-focusing system using electron ionization. 4-Dihexylaminostyrene[40] and diethyl 4-nitrophenylmethanephosphonate[28] were obtained by procedures described earlier. Tetrahydrofuran used for reactions was dried by stirring with Na metal overnight followed by degassing and vacuum transfer. HPLC was performed using a Shimadzu instrument equipped with a photodiode array detector. Reaction monitoring and separation were achieved with a nitro-derivatized silica HPLC column (ES Industries, catalog no. 138213-NO2) with the exception of the dibromodiformyl[2.2]paracyclophane mixture which was separated on a standard silica HPLC column. Quantitative HPLC analysis of the 2-fold donor coupling to **8** was performed by construction of 3-point calibration curves monitoring at 400 nm.

(4,7,12,15)-Tetra(bromomethyl)[2.2]paracyclophane (7). A 500 mL thick-walled Schlenk bomb with a wide-bore Teflon needle valve was charged with 7.2 g (34.5 mmol) of [2.2]paracyclophane and 20.7 g (690 mmol in formaldehyde) of paraformaldehyde with ∼150 mL of 33% HBr in glacial acetic acid. After tightly sealing the vessel, the mixture was sonicated at 60 °C for 5 days. The solids were collected and then extracted in three portions with 500 mL of $CHCl_3$ and washed with 500 mL of 1.0 M $CHCl_3$ in three portions. The crude yield was 44%. Purification was achieved by successive tritrations in warm $CHCl_3$, giving an off-white finely divided powder for a final yield of 4.1 g or 20%. ^{1}H NMR ($CDCl_3$): 6.596 (s, 4H), 4.324 (q, 8H), 3.441 (m, 4H), 2.932 (m, 4H). ^{13}C ($CDCl_3$): 138.463, 136.990, 133.765, 31.262, 31.066. HRMS-EI m/z = 578.8290, Δ = 1.4 ppm.

(4,7,12,15)-Tetra(diethylphosphonatemethyl)[2.2]paracyclophane (8). A 50 mL 14/20 round-bottom flask was charged with a Teflon-coated stir bar, 1.1 g (1.9 mmol) of **7**, 1.37 mL (8 mmol) of triethyl phosphite, and fitted with a short path distillation head with receiving flask. Argon was passed through the thermometer port and ran through an oil bubbler attached to the vacuum port. The reaction was heated to 120 °C for 2 h. The reaction was then cooled to ∼50 °C

(38) (a) Heller, A. *J. Chem. Phys.* **1964**, *40*, 2839. (b) Tachelet, W.; Jacobs, S.; Ndayikengurukiye, H.; Geise, H. J. *Appl. Phys. Lett.* **1994**, *64*, 2364. (c) Yang, Z.; Geise, H. J.; Mehbod, M.; Debrue, G.; Visser, J. W.; Sonneveld, E. J.; Van't dack, L.; Gijbels, R. *Synth. Met.* **1990**, *39*, 137. (d) Strehmel, B.; Sarker, A. M.; Malpert, J. H.; Strehmel, V.; Seifert, H.; Neckers, D. C. *J. Am. Chem. Soc.* **1999**, *121*, 1226.

(39) (a) Desiraju, G. R. *Angew. Chem., Int. Ed. Engl.* **1995**, *34*, 2311. (b) Thalladi, V. R.; Weiss, H.-H.; Bläser, D.; Boese, R.; Nangia, A.; Desiraju, G. R. *J. Am. Chem. Soc.* **1998**, *120*, 8702.

(40) Oprea, S.; Still, R. H. *J. Appl. Polym. Sci.* **1976**, *20*, 639.

and fitted with a thermometer and placed under vaccuum. Excess triethyl phosphite was removed under vacuum at 100 °C. The resulting oil was washed with several portions of pentane and diethyl ether affording a yellowish solid. The final yield was 98%. ^{1}H NMR ($CDCl_3$): 6.459 (s, 4H), 3.895 (m, 16H), 3.482 (m, 4H), 3.072 (m, 4H), 2.770 (m, 8H), 1.175 (q, 24H). ^{13}C ($CDCl_3$): 140.142, 138.762, 134.191, 131.089, 62.307, 32.300, 31.514, 16.532. HRMS-EI: 809.3120, $\Delta = 1.0$ ppm (for $M + H)^+$.

(4,7,12,15)-Tetra(4′-dihexylaminostyryl)[2.2]paracyclophane (1). A 25 mL 14/20 round-bottom flask was charged with 153.4 mg (0.19 mmol) of **8**, 275 mg (0.95 mmol) of 4-dihexylaminobenzaldehyde, a Teflon-coated stirbar, and closed with a septum. Approximately 5 mL of anhydrous DMF was added via syringe, and the mixture was stirred under argon at 0 °C. Deprotonation of the phosphonate was achieved with 96.5 mg (0.86 mmol) of potassium *t*-butoxide dissolved in a minimal amount of dry DMF added again by syringe. The reaction was allowed to warm to room temperature and stir overnight. The resulting mixture was extracted with hexanes (250 mL) and washed with three 250 mL portions of brine and then dried over $MgSO_4$. After filtration, the solvent was again reduced by rotary evaporation. Flash chromatography eluting with 10% diethyl ether in hexanes produced 243 mg of the product as an orange powder for a yield of 95%. Alternatively, the resulting orange oil from rotary evaporation was recrystallized twice in hexanes and afforded orange cube-shaped crystals of single-crystal X-ray diffraction quality for a final yield of 86% (214 mg). ^{1}H NMR ($CDCl_3$): 7.400 (d, 8H), 6.961 (m, 12H), 6.670 (d, 8H), 3.510 (m, 4H), 3.331 (t, 16H), 2.838 (m, 4H), 1.645 (m, 16H), 1.356 (m, 48H), 0.931 (m, 24H). ^{13}C NMR ($CDCl_3$): 147.774, 137.232, 136.781, 128.310, 128.106, 127.498, 125.641, 121.428, 111.872, 51.364, 33.316, 31.998, 27.574, 27.126, 22.945, 14.307. HRMS-FAB/NBA: 1349.1123, $\Delta = 3.3$ ppm.

4-(4′-Dihexylaminostyryl)-7,12,15-tri(4″-nitrostyryl)[2.2]-paracyclophane (2). A 25 mL 14/20 round-bottom flask was charged with 300 mg (0.37 mmol) of **8**, 110 mg (0.37 mmol) of 4-dihexylaminobenzaldehyde, a Teflon-coated stirbar, and closed with a septum. Approximately 5 mL of anhydrous DMF was added via syringe, and the mixture was stirred under argon at 0 °C. Deprotonation of the phosphonate was achieved with 45 mg (0.37 mmol) of potassium *t*-butoxide dissolved in a minimal amount of dry DMF. The reaction was allowed to warm to room temperature and stir overnight. Next, 170 mg (1.13 mmol) of 4-nitrobenzaldehyde in THF was added, and the reaction was again cooled to 0 °C. Another 1.2 mmol of potassium *t*-butoxide was added, and the reaction was allowed to proceed overnight. The resulting mixture was extracted with $CHCl_3$ (500 mL) and washed with three 500 mL portions of brine and then dried over $MgSO_4$. After filtration, the solvent was again reduced by rotary evaporation. Purification by HPLC afforded 235 mg of a black-metallic solid for a yield of 68%. ^{1}H NMR ($CDCl_3$): 8.275 (m, 6H), 7.567 (m, 6H), 7.376 (m, 4H), 7.135 (s, 1H), 7.006 (m, 4H), 6.92−6.83 (bm, 4H), 6.691 (d, 3H), 3.652 (m, 4H), 3.364 (t, 4H), 2.920 (m, 4H), 1.646 (m, 4H), 1.357 (m, 12H), 0.941 (t, 6H). ^{13}C NMR ($CDCl_3$): 148.510, 147.02, 146.882, 144.304, 144.078, 143.976, 139.308, 138.911, 138.743, 137.145, 136.824, 134.494, 130.339, 130.004, 129.745, 129.446, 129.148, 128.966, 128.678, 128.365, 128.103, 128.487, 127.298, 126.974, 126.741, 125.419, 124.636, 124.461, 124.173, 119.574, 111.839, 51.328, 33.622, 33.429, 33.054, 31.987, 31.852, 29.922, 27.552, 27.322, 27.078, 26.933, 22.938, 22.861, 14.300. HRMS-FAB/NBA: 934.4691, $\Delta = 2.3$ ppm.

(4,7)Bis(diethylphosphonatemethyl)-(12,15)bis(4′-dihexylaminostyryl)[2.2]paracyclophane (9). A 25 mL 14/20 round-bottom flask was charged with 50 mg (0.06 mmol) of **8**, 35 mg (0.12 mmol) of 4-dihexylaminobenzaldehyde, a Teflon-coated stirbar, and closed with a septum. Approximately 2 mL of anhydrous THF was added via syringe, and the mixture was stirred under argon at 0 °C. Deprotonation of the phosphonate was achieved with 13.4 mg (0.12 mmol) of potassium *t*-butoxide dissolved in a minimal amount of dry THF added again by syringe. The reaction was allowed to warm to room temperature and to progress overnight. The reaction was quenched with deionized water and extracted into 125 mL of $CHCl_3$ and washed with brine. The solvent was removed under vacuum, and the mixture was separated using HPLC. The resulting yield was 23%. Alternatively, reaction in DMF results in a 68% yield for the same procedure. The regiochemistry was assigned by characteristic paracyclophane fragmentation during mass spectrometry. ^{1}H NMR (CD_2Cl_2): 7.411 (d, 4H), 6.851 (m, 6H), 6.661 (d, 4H), 6.450 (s, 2H), 3.844 (m, 8H), 3.451 (m, 2H), 3.330 (m, 10H), 3.173 (m, 2H), 2.820 (m, 6H), 1.608 (t, 8H), 1.342 (m, 24H), 1.121 (m, 12H), 0.915 (m, 12H). ^{13}C NMR (CD_2Cl_2): 148.423, 138.712, 138.067, 137.475, 135.101, 130.716, 128.804, 128.242, 127.423, 125.276, 121.141, 112.159, 62.474, 51.557, 33.046, 32.887, 32.310, 32.052, 27.804, 27.348, 23.267, 16.674, 14.390. HRMS-ESI/TOF: 1079.71151, $\Delta = 1.2$ ppm for M^{+4}.

(4,12)Bis(diethylphosphonatemethyl)-(7,15)bis(4′-dihexylaminostyryl)[2.2]paracyclophane (10). A 25 mL 14/20 round-bottom flask was charged with 50 mg (0.06 mmol) of **8**, 35 mg (0.12 mmol) of 4-dihexylaminobenzaldehyde, a Teflon-coated stirbar, and closed with a septum. Approximately 2 mL of anhydrous THF was added via syringe, and the mixture was stirred under argon at 0 °C. Deprotonation of the phosphonate was achieved with 13.4 mg (0.12 mmol) of potassium *t*-butoxide dissolved in a minimal amount of dry DMF added again by syringe. The reaction was allowed to warm to room temperature and progress overnight. The reaction was quenched with deionized water and extracted into 125 mL of $CHCl_3$ washed with brine. The solvent was removed under vacuum, and the mixture was separated by HPLC. The resulting yield was 57% (37 mg). The regiochemistry was assigned by characteristic paracyclophane fragmentation during mass spectrometry combined with 2D ^{1}H NMR (COSY). ^{1}H NMR (CD_2Cl_2): 7.416 (d, 4H), 6.851 (m, 6H), 6.662 (d, 4H), 6.424 (d, 2H), 3.863 (m, 8H), 3.451 (m, 4H), 3.311 (t, 8H), 3.113 (m, 2H), 2.789 (m, 6H), 1.620 (m, 8H), 1.342 (m, 24H), 1.159 (m, 12H), 0.915 (t, 12H). ^{13}C NMR (CD_2Cl_2): 148.461, 138.848, 138.120, 137.832, 135.245, 129.980, 129.873, 129.107, 128.258, 127.355, 125.193, 121.301, 112.151, 62.565, 62.497, 51.557, 33.008, 32.871, 32.318, 31.627, 27.804, 27.348, 23.267, 16.750, 16.689, 16.636, 14.390. HRMS-ESI/TOF: 1079.71151, $\Delta = 1.8$ ppm for M^{+4}.

4,7-Bis(4′-dihexylaminostyryl)-12,15-bis(4″-nitrostyryl)[2.2]-paracyclophane (3). A 25 mL 14/20 round-bottom flask was charged with 0.5 mmol (540 mg) of **9**, 2.2 mmol of 4-nitrobenzaldehyde, a Teflon-coated stirbar, and was closed with a septum. Anhydrous DMF was added, and the reaction was cooled to 0 °C. Potassium *t*-butoxide (1.7 mmol) dissolved in a minimal amount of DMF was added via syringe, and the reaction was allowed to proceed for 24 h, warming slowly to room temperature. The resulting mixture was extracted with $CHCl_3$ (250 mL) and washed with three 250 mL portions of brine and then dried over $MgSO_4$. After filtration, the solvent was reduced by rotary evaporation. Purification by HPLC afforded 453.4 mg of a metallic-purple solid for a yield of 84%. ^{1}H NMR ($CDCl_3$): 8.252 (d, 4H), 7.589 (d, 4H), 7.363 (m, 6H), 7.121 (s, 2H), 7.001 (dd, 4H), 6.894 (s, 2H), 6.785 (d, 2H), 6.690 (d, 4H), 3.603 (m, 4H), 3.358 (t, 8H), 2.971 (m, 2H), 2.813 (m, 2H), 1.662 (m, 8H), 1.383 (m, 24H), 0.946 (t, 12H). ^{13}C NMR ($CDCl_3$): 147.892, 146.652, 144.136, 139.028, 136.753, 136.623, 136.530, 129.604, 128.439, 128.299, 127.814, 127.656, 127.003, 126.854, 124.496, 124.207, 120.143, 111.614, 51.102, 33.346, 32.954, 31.771, 27.325, 26.868, 22.720, 14.083. HRMS-EI: 1072.6818, $\Delta = 1.1$ ppm.

4,7,12-Tribromo-15-formyl[2.2]paracyclophane (13). A 100 mL 24/40 round-bottom flask was charged with 500 mg (0.95 mmol) of **12**[26] and a Teflon-coated stirbar and fitted with a needle valve. Approximately 50 mL of dry THF was transferred to the flask, and the reaction mixture was cooled to −78 °C. To the flask was added 1 equiv of *n*-butyllithium (0.95 mmol) via syringe through the needle

valve, which was allowed to react for 30 min, maintaining the reaction at −78 °C. Next, 8 equiv (∼1 mL) of anhydrous DMF was added via syringe, and the reaction was allowed to warm to room temperature. The reaction was quenched with a dilute ammonium hydroxide solution, and the THF was removed under vaccuum. The resulting solid was extracted with $CHCl_3$ (250 mL) and washed with three 250 mL portions of brine and then dried over $MgSO_4$. After filtration, the solvent was reduced by rotary evaporation. The resulting solid was coated onto 1.5 g of chromatographic silica and purified by flash chromatography (40 g column) with 3:2 $CHCl_3$:hexanes as eluent. A soapy white solid was recovered (166 mg, 37% yield). ^{1}H NMR ($CDCl_3$): 9.866 (s, 1H), 7.612 (s, 1H), 7.304 (s, 1H), 7.174 (s, 1H), 6.461 (s, 1H), 3.38−2.8 (bm, 8H). ^{13}C NMR ($CDCl_3$): 191.735, 143.241, 141.132, 140.662, 139.766, 137.270, 136.208, 135.852, 135.761, 134.099, 133.462, 125.678, 125.291, 34.722, 32.939, 32.780, 30.838. HRMS-EI: 473.001, Δ = 4.1 ppm.

4,7,12-Tris(4′-dihexylaminostyryl)-15-(4′′-nitrostyryl)[2.2]-paracyclophane (4). A 25 mL 14/20 round-bottom flask was charged with 392.6 mg (0.83 mmol) of **13**, 1.188 g (4.1 mmol) of 4-dihexylaminostyrene, 100 mg of tri-*o*-tolylphosphine, 60 mg of palladium acetate, 0.5 mL of triethylamine, and ∼5 mL of DMF, and was equipped with a Teflon-coated stirbar and a needle valve. The reaction mixture was degassed and was allowed to react at 100 °C overnight. The reaction was diluted with methylene chloride and the product extracted into methylene chloride (∼125 mL) and washed with three 125 mL portions of brine. The solution was dried with $MgSO_4$, filtered, and the solvent stripped. The resulting liquid was purified by flash chromatography (90 g column with 3:2 CH_2Cl_2:hexanes as eluent) for a total of 583 mg (64% yield) of 4-formyl-7,12,15-tris(4′-dihexylaminostyryl)[2.2]-paracyclophane (**14**). A second 10 mL round-bottom flask was charged with 338.6 mg (0.31 mmol) of **14**, 84.7 mg (0.31 mmol) of 4-nitrophenylmethanephosphonate, ∼2 mL of THF, a stirbar, and closed with a septum. The mixture was stirred and cooled to 0 °C. The phosphonate was deprotonated with 50 mg (0.43 mmol) of potassium *t*-butoxide, and the reaction was allowed to warm to room temperature and stir overnight. The reaction was diluted with methylene chloride and the product extracted into methylene chloride (∼125 mL) and washed with three 125 mL portions of brine. The solution was dried with $MgSO_4$, filtered, and the solvent removed in vacuo. The resulting liquid was purified by flash chromatography (90 g column with 3:7 CH_2Cl_2: hexanes as eluent) for a total yield of 81% (302 mg) of **4**. ^{1}H NMR ($CDCl_3$): 8.235 (d, 2H), 7.577 (d, 2H), 7.44−7.32 (bm, 6H), 7.064 (s, 1H), 7.02−6.74 (bm, 11H), 6.72−6.64 (m, 6H), 3.62−3.48 (m, 4H), 3.332 (t, 12H), 2.98−2.74 (m, 4H), 1.653 (s, 12H), 1.360 (m, 48H), 0.924 (m, 18H). ^{13}C NMR ($CDCl_3$): 148.124, 148.004, 147.909, 146.514, 144.985, 139.297, 139.046, 137.534, 137.185, 136.897, 136.879, 136.879, 136.624, 134.614, 130.539, 130.047, 128.747, 128.416, 128.186, 128.099, 127.968, 127.844, 127.702, 127.542, 126.941, 125.419, 125.346, 125.047, 124.410, 120.973, 120.874, 120.605, 111.890, 111.847, 111.814, 51.353, 33.808, 33.327, 33.149, 31.998, 27.566, 27.111, 27.104, 22.942, 14.304. HRMS-FAB/NBA: 1210.8943, Δ = 0.1 ppm.

4,15-Dibromo-7,12-diformyl[2.2]paracyclophane (16) and 4,12-Dibromo-7,15-diformyl[2.2]paracyclophane (17). A 100 mL 24/40 round-bottom flask was charged with 618.1 mg (1.18 mmol) of **12** and a Teflon-coated stirbar and fitted with a needle valve. Approximately 50 mL of dry THF was transferred to the flask, and the reaction mixture was cooled to −78 °C. To the flask was added 1.1 mL of a 2.3 M *n*-butyllithium solution (2.48 mmol) via syringe through the needle valve, which was allowed to react for 30 min. Next, 8 equiv (∼1 mL) of anhydrous DMF was added via syringe, and the reaction was allowed to warm to room temperature. The reaction was quenched with a dilute ammonium hydroxide solution, and the THF was removed under vacuum. The resulting solid was extracted with $CHCl_3$ (250 mL) and washed with three 250 mL portions of brine and then dried over $MgSO_4$. After filtration, the solvent was again reduced by rotary evaporation. GC/MS analysis showed two close peaks with the expected product mass of 420. Both revealed a major fragment at 210, characteristic of the isomers identified as **16** and **17**. These were separated successfully with HPLC to yield 55% of **16** and 34% of **17**. None of 4,7-dibromo-12,15-diformyl-[2.2]paracyclophane (**15**) was identified from GCMS. The absolute spatial assignment was achieved by 2D ^{1}H COSY. The disposition of the C_2 axis of symmetry for **16** allows for coupling between all of the inequivalent methylene protons found on the paracyclophane bridgeheads. Analogous coupling is not possible for **17** where the protons on the two bridging carbons on one side of the molecule are related by symmetry. All proton resonances are coupled in the COSY of **16**, while there are uncoupled methylene resonances for **17**. For **16**, ^{1}H NMR ($CDCl_3$): 9.802 (s, 2H), 7.286 (s, 2H), 6.894 (s, 2H), 3.950 (m, 2H), 3.499 (m, 2H), 3.050 (m, 4H). ^{13}C NMR ($CDCl_3$): 191.332, 143.620, 140.290, 137.551, 136.087, 135.639, 133.189, 35.132, 30.679. HRMS-EI: 419.539, Δ = 1.2 ppm. For **17**, ^{1}H NMR ($CDCl_3$): 9.910 (s, 2H), 7.592 (s, 2H), 6.608 (s, 2H), 4.051 (m, 2H), 3.393 (m, 2H), 3.189 (m, 2H), 2.918 (m, 2H). ^{13}C NMR ($CDCl_3$): 191.469, 143.886, 139.956, 138.674, 135.579, 134.759, 133.644. HRMS-EI: 419.539, Δ = 0.4 ppm.

4,15-Bis(4′-dihexylaminostyryl)-7,12-bis(4′′-nitrostyryl)[2.2]-paracyclophane (5) and 4,12-Bis(4′-dihexylaminostyryl)-7,15-bis-(4′′-nitrostyryl)[2.2]paracyclophane (6). Because the preparations of **5** and **6** are identical, only the synthesis of **5** is reported as an example. A 25 mL 14/20 round-bottom flask was charged with 110 mg (0.26 mmol) of **16**, 290 mg (1.04 mmol) of 4-dihexylaminostyrene, 50 mg of tri-*o*-tolylphosphine, 50 mg of palladium acetate, 0.5 mL of triethylamine, and ∼3 mL of DMF, and was equipped with a Teflon-coated stirbar and a needle valve. The reaction mixture was degassed and was allowed to react at 100 °C overnight. The reaction was diluted with methylene chloride and the product extracted into methylene chloride (∼500 mL) and washed with three 500 mL portions of deionized water. The solution was dried with $MgSO_4$, filtered, and the solvent removed. The resulting liquid was purified by flash chromatography (90 g column with 75% CH_2Cl_2/25% hexanes as eluent) for a total yield of 93% of 7,12-diformyl-4,15-bis(4-dihexylaminostyryl)-[2.2]paracyclophane (**18**). A second 5 mL round-bottom flask was charged with 97 mg (0.1 mmol) of **18**, 68.3 mg (0.25 mmol) of 4-nitrophenylmethanephosphonate, ∼2 mL of THF, a stirbar, and closed with a septum. The mixture was stirred and cooled to 0 °C. The phosphonate was deprotonated with 28 mg (0.25 mmol) of potassium *t*-butoxide, and the reaction was allowed to warm to room temperature and stir overnight. The reaction was diluted with methylene chloride and the product extracted into methylene chloride (∼500 mL) and washed with three 500 mL portions of deionized water. The solution was dried with $MgSO_4$, filtered, and the solvent removed in vacuo. The resulting liquid was purified by flash chromatography (90 g column with 40% CH_2Cl_2/60% hexanes as eluent) for a total yield of 79% (85 mg) of **5**. An alternate preparation of **6** is reaction of **10** with 4-nitrobenzaldehyde in a procedure identical to the preparation of **3** for a yield of 92%. For **5**, ^{1}H NMR ($CDCl_3$): 8.268 (d, 4H), 7.549 (d, 4H), 7.398 (m, 6H), 6.964 (m, 10H), 6.676 (d, 4H), 3.604 (m, 4H), 3.350 (t, 8H), 2.842 (m, 4H), 1.655 (m, 8H), 1.363 (m, 24H). ^{13}C NMR ($CDCl_3$): 148.353, 146.649, 144.694, 139.177, 138.656, 137.458, 134.687, 130.120, 129.865, 128.496, 128.277, 128.081, 126.999, 125.794, 124.465, 124.421, 120.044, 111.839, 51.328, 33.600, 33.145, 31.991, 27.559, 27.086, 22.938, 14.300. HRMS-FAB/NBA: 1072.6765, Δ = 3.8 ppm. For **6**, ^{1}H NMR ($CDCl_3$): 8.239 (d, 4H), 7.565 (d, 4H), 7.372 (m, 6H), 6.958 (10H), 6.689 (d, 4H), 3.595 (m, 4H), 3.362 (t, 8H), 2.845 (m, 4H), 1.645 (m, 8H), 1.383 (m, 24H), 0.969 (t, 12H). ^{13}C NMR ($CDCl_3$): 148.266, 146.740, 144.584, 139.461, 139.097, 137.192, 134.403, 130.477, 130.411, 128.893, 128.500, 127.684, 126.682, 125.033, 124.752, 124.603, 120.160, 111.788, 51.388, 33.823, 33.021, 31.987, 27.555, 27.104, 22.934, 14.300. HRMS-FAB/NBA: 1072.6794, Δ = 1.1 ppm.

Acknowledgment. Financial support from the National Science Foundation (DMR 0097611) and the Office of Naval Research is gratefully acknowledged. The authors would like to thank Dr. Xianhui Bu for assistance with crystallography and for useful discussions.

Supporting Information Available: Complete experimental details of the X-ray crystallographic determination of **7**, DD, **1**, and **3** (PDF). This material is available free of charge via the Internet at http://pubs.acs.org.

JA0121383